

Chaotic Cryptographic Scheme Based on Composition Maps

S. Behnia ^{a*}, M.A. Jafarizadeh ^b, A. Akhshani ^a, H. Mahmodi ^a
and A. Akhavan ^c

^aDepartment of Physics, IAU, Urmia, Iran.

^bDepartment of Theoretical Physics and Astrophysics, Tabriz University, Tabriz, Iran.

^cFaculty of Engineering, IAU, Urmia, Iran.

December 2, 2024

Abstract

In recent years, a growing number of cryptosystems based on chaos have been proposed. But most of them encountered more problems such as small key space and weak security. Based on such a fact, in the present report, a new kind of chaotic cryptosystem based on Composition of Trigonometric Chaotic Maps (*CTCMs*) is proposed. In the new scheme employs the composition map to shuffle the positions of the image pixels and uses the another chaotic map to confuse. Both theoretical and experimental results indicate that the encryption algorithm based on *CTCMs* shows advantages of large key space to resist the brute force attack and high level of security.

Keywords: Chaos Theory, Chaotic Cryptosystem, Composition Map, Encryption, Security.

PACsnumbers: 05.45.Vx

*E-mail: S.behnia@iaurmia.ac.ir

1 Introduction

Chaos theory is established since 1970s from many different research areas, such as physics, mathematics, biology, engineering and chemistry, etc. [1]. Chaotic systems have a number of interesting properties such as ergodicity, the sensitive dependence on initial conditions, system parameters, mixing, etc. Most properties are related to some requirements such as confusion and diffusion for constructing the cryptosystems. Many researchers have pointed out that there exists tight relationship between chaos and cryptography [2, 3, 4, 5]. Recently there has been a great interest in developing secure communication schemes utilizing chaos. There exist two main approaches of designing chaos-based cryptosystems: analog mode and digital mode. From 1989, together with the use of analog chaotic systems in the design of secure communication systems [6, 7, 8, 9, 10, 11], applications of computerized (also called digital) chaotic systems in cryptography have attracted more and more attention. This paper chiefly focuses on the digital chaotic ciphers. In the digital world nowadays, the security of digital images becomes more important since the communications of digital products over network occur more and more frequently. Thus, to protect the content of digital images, some specific encryption systems are needed. The ideas of using digital chaotic systems to construct cryptosystems have also been proposed [12, 13, 14, 15, 16, 17, 18, 19, 20, 21]. Due to some intrinsic features of images, such as bulk data capacity and high correlation among pixels, traditional encryption algorithms such as DES, IDEA and RSA are not suitable for practical image encryption, especially under the scenario of on-line communications. The main obstacle in designing image encryption algorithms is that it is rather difficult to swiftly permute and diffuse data by traditional means of cryptology. In this respect, chaos-based algorithms have shown their superior performance. Because of the advantages of high-level efficiency and simplicity of one-dimensional chaotic systems [22], some of the researches in image encryption algorithms based on chaotic systems such as Logistic map have been widely used now, but it is obvious that the drawbacks of small key space and weak security

in one-dimensional chaotic cryptosystems [23, 24].

To eliminate these drawbacks, the objective of this Letter is to introduce a new chaotic algorithm which has the advantages of high-level security and large key space, hence we present algorithm based on Trigonometric Chaotic Maps [25] and for increasing security we used Composition of Trigonometric Chaotic Maps so called *CTCMs* [26]. Since digital images are usually represented as two-dimensional arrays, so we applied these kind of maps in two direction of image. Meanwhile, to confuse the relationship between cipher-image and plain-image, a diffusion process among pixels is performed. We have shown that by taking advantage of the exceptionally good properties of *CTCMs* such as mixing, sensitivity to initial conditions and system parameters, the proposed scheme incorporates *CTCMs* alternatively uses permutation and diffusion to render the image totally unrecognizable. Theoretical and experimental results indicate that the encryption algorithm based on *CTCMs* is advantageous from the point of view of large key space and high security.

The remaining of the Letter is organized as follows. A new chaotic algorithm is introduced briefly in section 2. In section 3 presents the encryption algorithm based on *CTCMs*. Section 4 Some experimental results for verification. In Section 5, security of the chaotic encryption algorithm is discussed. Finally, Section 6 concludes the paper.

2 A New Scheme Based on *CTCMs*

2.1 Many-Parameters Families of Chaotic Maps

Let us first consider the one-parameter families of chaotic maps of the interval $[0, \infty)$ defined as follows [25]:

$$\Phi_N^{(1)}(x, \alpha) = \frac{1}{\alpha^2} \tan^2(N \arctan \sqrt{x}), \quad (2-1)$$

$$\Phi_N^{(2)}(x, \alpha) = \frac{1}{\alpha^2} \cot^2(N \arctan \frac{1}{\sqrt{x}}). \quad (2-2)$$

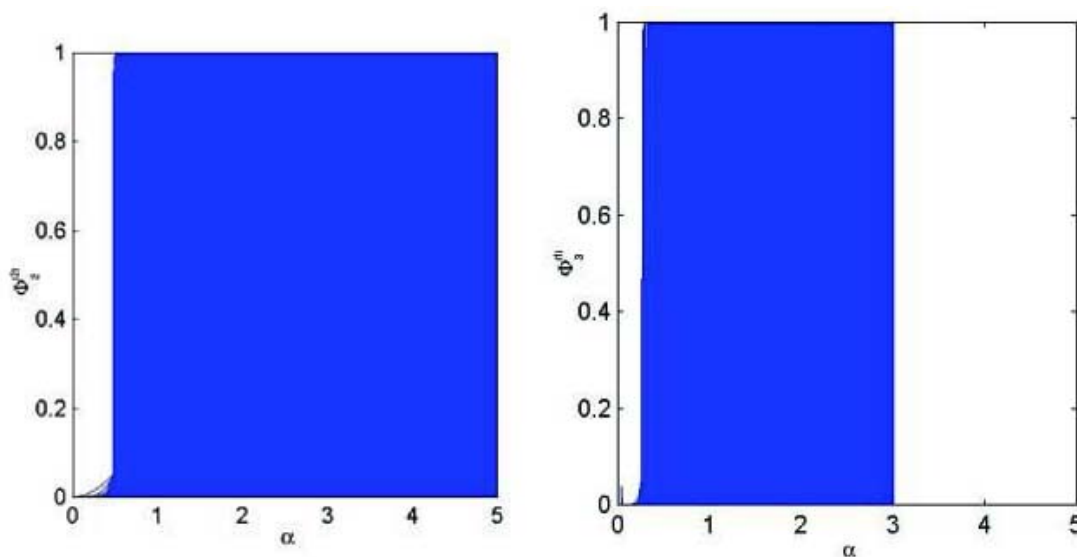


Figure 1: bifurcation

where N is an integer greater than one. By considering the invertible map $g(x) = g^{-1}(x) = 1 - x$ one could related this two family of chaotic maps as follows:

1- $\Phi_N^{(1)}(x, \alpha) = g(\Phi_N^{(2)}, g(x), \frac{1}{\alpha}) = g \circ \Phi_N^{(1)}(\frac{1}{\alpha}) \circ g(x)$ for even N

2- $\Phi_N^{(1)}(x, \alpha) = \Phi_N^{(2)}(x, \alpha)$ for odd N

These maps have interesting property, that is, for even values of N the $\Phi^{(1)}(\alpha, x)(\Phi^{(2)}(\alpha, x))$ maps have only a fixed point attractor $x = 1(x = 0)$ provided that their parameter belongs to interval $(N, \infty)((0, \frac{1}{N}))$ while, at $\alpha \geq N (\alpha \geq \frac{1}{N})$ they bifurcate to chaotic regime without having any period doubling or period-n-tupling scenario and remain chaotic for all $\alpha \in (0, N) (\alpha \in (\frac{1}{N}, \infty))$ but for odd values of N , these maps have only fixed point attractor $x = 0$ for $\alpha \in (\frac{1}{N}, N)$, again they bifurcate to chaotic regime at $\alpha \geq \frac{1}{N}$, and remain chaotic for $\alpha \in (0, \frac{1}{N})$, finally they bifurcate at $\alpha = N$ to have $x = 1$ as fixed point attractor for all $\alpha \in (\frac{1}{N}, \infty)$ (see Fig. 1). From now on, depending on the situation we will consider one of these maps (2-1), (2-2). Using the above hierarchy of family of

one-parameter chaotic maps we can generate new hierarchy of families of many-parameters chaotic maps with an invariant measure [26] simply from the composition of these maps.

Hence considering the functions $\Phi_{N_k}(x, \alpha_k), k = 1, 2, \dots, n$ we denote their composition by: $\Phi_{N_1, N_2, \dots, N_n}^{\alpha_1, \alpha_2, \dots, \alpha_n}(x)$ which can be written in terms of them in the following form:

$$\Phi_{N_1, \dots, N_n}^{\alpha_1, \dots, \alpha_n}(x) = \overbrace{(\Phi_{N_1} \circ \dots \circ \Phi_{N_n}(x))}^n = \Phi_{N_1}(\Phi_{N_2}(\dots(\Phi_{N_n}(x, \alpha_n), \alpha_{(n-1)})\dots), \alpha_2), \alpha_1)$$

or

$$\Phi_{N_1, N_2, \dots, N_n}^{\alpha_1, \alpha_2, \dots, \alpha_n}(x) = \frac{1}{\alpha_1^2} \tan^2 \left(N_1 \arctan \sqrt{\frac{1}{\alpha_2^2} \tan^2(N_2 \arctan \sqrt{\dots \frac{1}{\alpha_n^2} \tan^2(N_n \arctan \sqrt{x}) \dots})} \right). \quad (2-3)$$

one can show that the chaotic regions is [26]: $\prod_{k=1}^n \frac{1}{N_k} < \prod_{k=1}^n \alpha_k < \prod_{k=1}^n N_k$ for odd integer values of N_1, N_2, \dots, N_n and if one of the integers happens to become even, then the chaotic region in the parameter space is defined by $\alpha_k > 0, \text{ for } k = 1, 2, \dots, n$ and $\prod_{k=1}^n \alpha_k < \prod_{k=1}^n N_k$ if one of the integers happens to become even, respectively. Out of these regions they have only period one stable fixed points.

2.2 Lyapunov Characteristic Exponent

In order to investigate these maps numerically, we try to calculate Lyapunov characteristic exponent of maps $\Phi_{N_1, N}^{\alpha_1, \alpha_2}(x)$. In fact, Lyapunov characteristic exponent is the characteristic exponent of the rate of average magnificent of the neighborhood of an arbitrary point x_0 and it is denoted by $\lambda_{N_1, N_2, \dots, N_n}^{\alpha_1, \alpha_2, \dots, \alpha_n}(x_0)$ which is written as:

$$\begin{aligned} \lambda_{N_1, N_2, \dots, N_n}^{\alpha_1, \alpha_2, \dots, \alpha_n}(x_0) &= \lim_{n \rightarrow \infty} \ln \left| \frac{d}{dx} \overbrace{\Phi_{N_1, N_2, \dots, N_n}^{\alpha_1, \alpha_2, \dots, \alpha_n}(x, \alpha) \circ \Phi_{N_1, N_2, \dots, N_n}^{\alpha_1, \alpha_2, \dots, \alpha_n} \dots \circ \Phi_{N_1, N_2, \dots, N_n}^{\alpha_1, \alpha_2, \dots, \alpha_n}}^n \right| \\ &= \lim_{n \rightarrow \infty} \frac{1}{n} \sum_{k=0}^{n-1} \ln \left| \frac{d\Phi_{N_1, N_2, \dots, N_n}^{\alpha_1, \alpha_2, \dots, \alpha_n}(x_k, \alpha)}{dx} \right|, \end{aligned} \quad (2-4)$$

where $x_k = \overbrace{\Phi_{N_1, N_2, \dots, N_n}^{\alpha_1, \alpha_2, \dots, \alpha_n} \circ \Phi_{N_1, N_2, \dots, N_n}^{\alpha_1, \alpha_2, \dots, \alpha_n} \circ \dots \circ \Phi_{N_1, N_2, \dots, N_n}^{\alpha_1, \alpha_2, \dots, \alpha_n}}^k$. It is obvious that

- 1- $\lambda_{N_1, N_2, \dots, N_n}^{\alpha_1, \alpha_2, \dots, \alpha_n}(x_0) < 0$ for an attractor,
- 2- $\lambda_{N_1, N_2, \dots, N_n}^{\alpha_1, \alpha_2, \dots, \alpha_n}(x_0) > 0$ for a repeller
- 3- $\lambda_{N_1, N_2, \dots, N_n}^{\alpha_1, \alpha_2, \dots, \alpha_n}(x_0) = 0$ for marginal situation

Also the Lyapunov number is independent of initial point x_0 , provided that the motion inside the invariant manifold is ergodic, thus $\lambda_{N_1, N_2, \dots, N_n}^{\alpha_1, \alpha_2, \dots, \alpha_n}(x_0)$ characterizes the invariant manifold of $\Phi_{N_1, N_2, \dots, N_n}^{\alpha_1, \alpha_2, \dots, \alpha_n}$ as a whole. For the values of parameters $\alpha_k, k = 1, 2, \dots, n$, where the map $\Phi_{N_1, N_2, \dots, N_n}^{\alpha_1, \alpha_2, \dots, \alpha_n}$ is measurable, Birkhoff ergodic theorem implies the equality of KS-entropy and Lyapunov characteristic exponent, that is:

$$h(\mu, \Phi_{N_1, N_2, \dots, N_n}^{\alpha_1, \alpha_2, \dots, \alpha_n}) = \lambda_{N_1, N_2, \dots, N_n}^{\alpha_1, \alpha_2, \dots, \alpha_n}(x_0). \quad (2-5)$$

Therefore, combining the analytic discussions with the numerical simulation we deduce that these maps are ergodic in certain region of their parameters space as explained above and in the complementary region of the parameters space they have only a single period one attractive fixed point, such that in contrary to the most of usual one-dimensional one-parameter or many-parameters family of maps they have only a bifurcation from a period one attractive fixed point to chaotic state or vice-versa.

3 Encryption Algorithm Based on *CTCMs*

In chaos theory, Kolmogorov entropy is defined to measure the decreasing rate of the information. Since in one-dimensional chaotic maps, Kolmogorov entropy is equal to Lyapunov exponent Eq. (2-5), and also a possible way to describe the key space might be in terms of positive Lyapunov exponents so we choose a chaotic region for *CTCMs* (see Fig. 2). Here in this Letter we give a new hierarchy of many -parameter families of maps of the interval $[0, \infty)$ for encryption/decryption process. In designing this algorithm for image encryption, we used Eq. (2-1) and (2-2) to construct composition forms of these maps and

obtained Eq. (3-6) and (3-7) where $N_1=3$, $N_2=5$ in Eq. (3-6) and $N_1=4$, $N_2=8$ in Eq. (3-7) also for distinguish between control parameters in two equations, α' is used instead of α in Eq. (3-7). The image encryption algorithm is based on the Composition of Trigonometric Maps (*CTCMs*) for image $I_{m \times n}$, $m \times n$ pixels, are presented in four steps which is based on *Permutation* and XOR-ing processes by using Eq. (3-6) and (3-7), respectively.

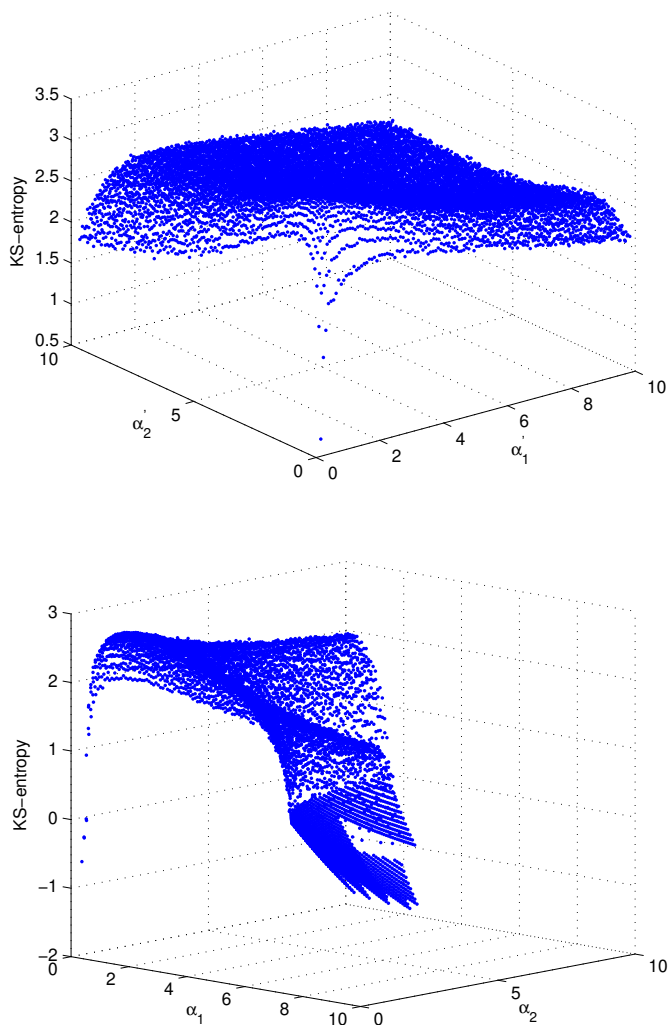


Figure 2: KS-entorpy

$$\Phi_{N_1, N_2}^{\alpha_1, \alpha_2} = \frac{1}{\alpha_2^2} \tan^2 \left(N_2 \arctan \left(\sqrt{\frac{(\tan^2 (N_1 \arctan (\sqrt{x})))}{\alpha_1^2}} \right) \right) \quad Type I \quad (3-6)$$

$$\Phi_{N_1, N_2}^{\alpha'_1, \alpha'_2} = \frac{1}{\alpha'_2} \cot^2 \left(N_2 \arctan \left(\frac{1}{\sqrt{\frac{(\cot^2 (N_1 \arctan (\frac{1}{\sqrt{x}})))}{\alpha'_1{}^2}}} \right) \right) \quad Type II \quad (3-7)$$

Permutation and XOR-ing parameters are as follows:

$$Permutation : \begin{cases} m : N, & x_0, & \alpha_{1x}, & \alpha_{2x}, \\ n : N, & y_0, & \alpha_{1y}, & \alpha_{2y}, \end{cases}, \text{ XOR-ing} = \begin{cases} m \times n : \alpha_1, & \alpha_2, & x_0, & N \end{cases}$$

$$XOR - ing : \begin{cases} m \times n : N, & x_0, & \alpha'_{1x}, & \alpha'_{2x} \end{cases}$$

Step 1: Permute image $I_{m \times n}$ pixels using chaotic map *CTCM I* and store results in $P_{m \times n}$.

Step 2: Using chaotic map *CTCM I* and following formula change pixels values and store new values in C_k :

$$X_k = \{ \text{floor}(x \times 10^{14}) \} \quad \text{mod} \quad 256 \quad (3-8)$$

$$C_{ij} = X_k \text{ XOR } \{(P_{ij} + X_k) \text{ mode } 256\} \text{ XOR } C_p$$

where C_p modified previous pixel. In decryption process the above formulas inverse is like:

$$P_{ij} = \{X_k \text{ XOR } C_p \text{ XOR } C_{ij} + 256 - X_k\} \text{ mod } 256$$

Step 3: Do XOR operation on C using chaotic map *CTCM II* following formula and same encrypted

$$E_{ij} = \{ \text{floor}(x_{ij} \times 10^{14}) \text{ mod } 256 \} \text{ XOR } C_{ij} \quad (3-9)$$

The decryption algorithm is similar to the encryption algorithm but receiving encryption key and operating with the encrypted image.



Figure 3: (a)plain-image,(b)ciphered image

4 Experimental Results

To evaluate the efficiency of the proposed cryptographic scheme based on *CTCMs*, we give some experimental results in this section. Experimental analysis of the new algorithm presented in this Letter has been done with an indexed image 'Boat' of size 256×256 is used as a plain-image, see Fig. 3(a). Our experimental tests indicate that the running speed of the proposed algorithm is acceptable. The proposed algorithm is implemented using Visual C++ running in the personal computer with 2.4 GHz Pentium IV, 512 Mb memory and 80 G hard-disk capacities. The average time used in encryption/decryption on 256 grey-scale images of size 256×256 is shorter than 0.5s.

As we can see in Fig. 5(a) and (b), the decrypted image with wrong keys $x_0=2.10155400000001$ in permutation and $\alpha'_1=61.52200000000005$ in XOR-ing has a histogram with random behavior. The sensitivity to initial conditions which is the main characterization of chaos guarantees the security of our scheme. Undoubtedly, the secret keys are secure enough even a chosen plaintext/ciphertext attack is adopted.

$$Permutation = \begin{cases} x : \left\{ \alpha_1 = 2.10155, \alpha_2 = 3.569221, x_0 = 25.687, N_x = 950 \right. \\ y : \left\{ \alpha_1 = 1.8874, \alpha_2 = 4.23562, y_0 = 574.461, N_y = 750 \right. \end{cases}$$

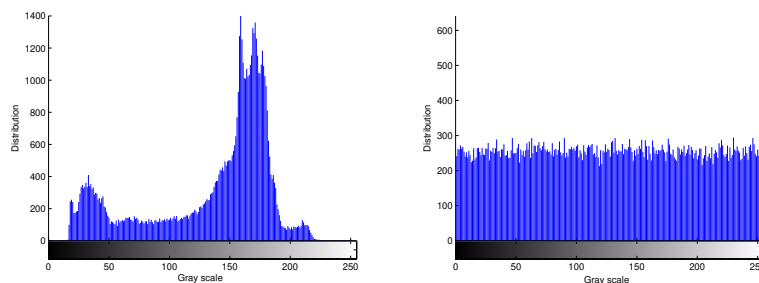


Figure 4: (a) histogram of plain-image, (b) histogram of ciphered-image,

$$XOR - ing = \left\{ m \times n : \alpha_1 = 2.8912, \alpha_2 = 3.89954, x_0 = 814.217217, N = 1200 \right.$$

$$XOR - ing = \left\{ m \times n : \alpha'_1 = 61.522, \alpha'_2 = 257.26223, x_0 = 79.82, N = 800 \right.$$

A number of experiments proves that the new algorithm validly solves problem of encryption failure owing to the small key space and weak security.

Statistical analysis has been performed on the proposed image encryption algorithm, demonstrating its superior confusion and diffusion properties which strongly resist statistical attacks. One typical example among them is shown in Fig. 4(a) and (b). From the figure, one can see that the histogram of the ciphered image is fairly uniform and is significantly different from that of the original image.

5 Security Analysis

A good encryption scheme should resist all kinds of known attacks, such as known-plain-text attack, cipher-textonly attack, statistical attack, differential attack, and various brute-force attacks. Some security analysis has been performed on the proposed image encryption scheme, including the most important ones like key space analysis, information entropy and statistical analysis which has demonstrated the satisfactory security of the new scheme, as demonstrated in the following.

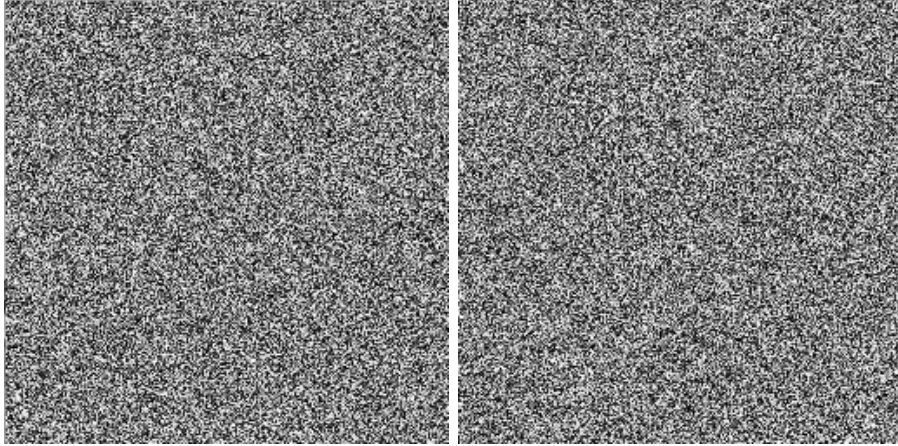


Figure 5: (a)the decrypted image with wrong key of Permutation, (b)the decrypted image with wrong key of XOR-ing

5.1 Key space analysis

Key space size is the total number of different keys that can be used in the encryption. As mentioned above, the key of the cryptosystem is composed of three parts: permutation parameters, XOR-ing (I) and XOR-ing (II) parameters which consists of 8 control parameters, 4 initial conditions and 4 iteration numbers. Cryptosystem is completely sensitive to all secret keys see Fig. 5(a) and (b). If the precision is 10^{-14} , the key space size for just initial conditions is $10^{14 \times 4} = 10^{56} \approx 2^{186}$. moreover, all of the control parameters and iteration numbers are used as secret keys. Therefore the key space is very large to resist all kinds of brute-force attacks.

5.2 Information Entropy

It is well known that the entropy H of a symbol source S can be calculated as:

$$H(S) = \sum_{i=0}^{2^N-1} P(s_i) \log \frac{1}{P(s_i)} \text{bits}, \quad (5-10)$$

where $P(s_i)$ represents the probability of symbol s_i and \log represents the base 2 logarithm so that the entropy is expressed in bits. Actually, given that a real information source seldom transmits random messages, in general the entropy value of the source is smaller than the ideal one.. However, when these messages are encrypted, their entropy should ideally be 8. If the output of such a cipher emits symbols with entropy less than 8, then there exists a predictability which threatens its security [29].

$$H(S) = \sum_{i=0}^{255} P(s_i) \log \frac{1}{P(s_i)} \text{bits} = 7.997 \approx 8$$

The value obtained is very close to the theoretical value 8. This means that information leakage in the encryption process is negligible and the encryption system is secure upon the entropy attack. The ciphertext entropy for various values of s is calculated using Eq. (3-8) and is listed in Table 1. Compared with the existing algorithms, such as [27, 28, 29], the proposed algorithm is more better.

5.3 Correlation of two adjacent pixels

To test the correlation between two adjacent pixels in plain-image and ciphered image, the following procedure was carried out. Randomly select 1000 pairs of two adjacent (in vertical, horizontal, and diagonal direction) pixels from plain-images and ciphered image, and calculate the correlation coefficients [30], respectively (see Table 2 and Fig. 6) by using the following two formulas:

$$E(x) = \frac{1}{N} \sum_{i=1}^N x_i, \quad (5-11)$$

$$D(x) = \frac{1}{N} \sum_{i=1}^N (x_i - E(x))^2, \quad (5-12)$$

$$\text{cov}(x, y) = \frac{1}{N} \sum_{i=1}^N (x_i - E(x))(y_i - E(y)), \quad (5-13)$$

$$r_{xy} = \frac{\text{cov}(x, y)}{\sqrt{D(x)}\sqrt{D(y)}} \quad (5-14)$$

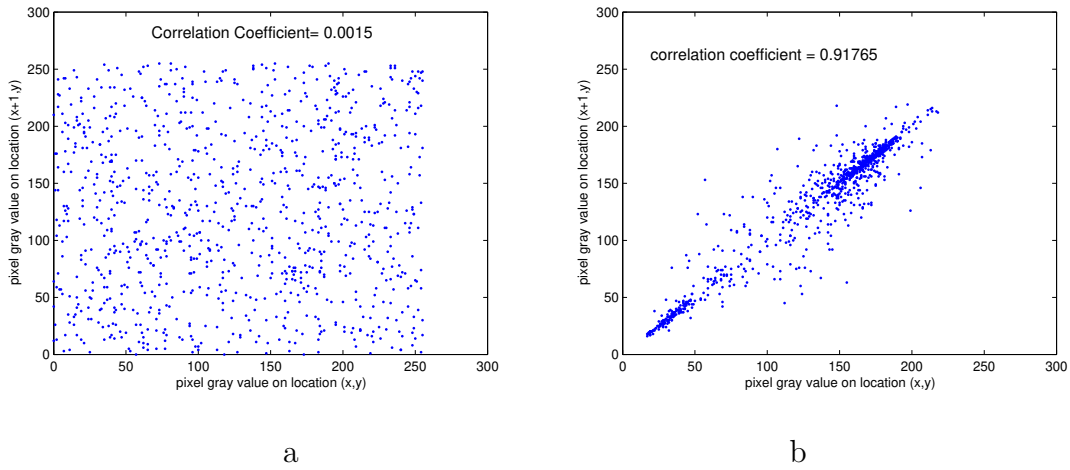


Figure 6: Correlations of two horizontally adjacent pixels in the plain-image and in the cipher-image: (a)correlation analysis of plain- image,(b)correlation analysis of cipher-image

Where, $E(x)$ is the estimation of mathematical expectations of x , $D(x)$ is the estimation of variance of x , and $cov(x, y)$ is the estimation of covariance between x and y . where x and y are grey-scale values of two adjacent pixels in the image.

Table 1: Entropy value for the ciphertext of different sources s

s	256
Ideal	8
Baptista's	7.926
Wong's	7.969
Xiang's	7.995
Proposed	7.997

Table 2: Correlation coefficients of two adjacent pixels in two images

	Plain image	Ciphered image
Horizontal	0.9525	0.0023
vertical	0.9443	-0.0024
Diagonal	0.9066	0.0013

6 Conclusion

In this letter, we point out two essential defects existing in the chaotic encryption scheme proposed in [23, 24], and propose a new scheme based on the hierarchy of one dimensional chaotic maps of interval $[0, \infty)$. These maps which are defined as ratios of polynomials of degree N have interesting property such as invariant measure, Ergodicity, variable control parameters in the two interval; $[\frac{1}{N}, N]$ for odd N and $[\frac{1}{N}, \infty)$ for even N , Capability of calculation KS-entropy and ability to construct composition form of maps [26]. In this algorithm, the chaotic properties such as mixing and sensitive dependence on initial conditions and control parameters are suitably utilized while the limitation and weaknesses of the chaotic encryption system are effectively overcome. In our scheme employs the chaotic map (*CTCM I*) to shuffle the positions of image pixels and uses another chaotic map (*CTCM II*) to confuse the relationship between cipher-image and plain-image, thereby significantly increasing its resistance to various attacks such as the statistical and differential attacks. Our experiments show that even a simple algorithm can achieve a good estimation and also acceptable encryption speed. We conclude inclusion of composition map increases the confusion in the encryption process and it results in a more secure cryptosystem due to the fact that more confusion in encryption makes cryptosystem more secure. The analysis indicates that the algorithm can satisfy all the performance requirements such as high level of security and large key space. Furthermore, the entropy measured is almost equal to the ideal value. It is practicable and reliable, with high potential to be adopted for Internet image encryption, transmission applications, secure communication and other information security fields.

References

- [1] H. BAI-LIN *Shanghai Scientific and Technological Education Publishing House*, Shang-

hai, China, (1993).

- [2] R. BROWN, L.O. CHUA, *Int.J.Bifur. Chaos* 6(2) (1996), pp.219-242.
- [3] L. KOCAREV, G. JAKIMOSKI, U. PARLITZ, *in Proc.IEEE Int.Symposium Circuits and Systems 4* (1998), pp.514-517.
- [4] G.ALVAREZ, F. MONOTOYA, G. PASTOR, M. ROMERA, *in Proc.IEEE Int.Carnahan Conf.Securiyt Technology* ,(1998).
- [5] J. FRIDRICH. *Int. J. Bifro. Chaos* 8(6)(1998), pp.1259-1284.
- [6] G. ALVAREZ, F. MONOTOYA, M. ROMERA, *Technology, IEEE*, (1999), pp.332-338.
- [7] H. ZHOU, X. LING. *IEEE Trans. Circuits Syst. I*, 44 (1997 b), pp.268-271.
- [8] Y.-C. LAI, E. BOLLT, C. GREBOGI, *Phys. Lett. A* 255 (1999), pp.75-81.
- [9] Q.MEMON, *Comp.Comm.* 26 (2003), pp.498-505.
- [10] U. PARLITZ, L.O. CHUA, L. KOCAREV, K.S. HALLE, A. SHANG, *Int. J. Bifur. Chaos* 2 (1992), pp.973-977.
- [11] J.Y. CHEN, K.W. WONG, L.M. CHENG, J.W. SHUAI,, *Chaos* 13 (2003), pp.508-514.
- [12] M.S. BAPTISTA, *Phys. Lett. A* 240 (1998), pp.50-54.
- [13] Z. HONG, L. XIETING, *Int. J.Bifur. Chaos* 7(1) (1997), pp.205-213.
- [14] G. JAKIMOSKI, L. KOCAREV, *IEEE Trans.Circuits and Systems I*, 48(2) (2001a), pp.163-169.
- [15] N. MASUDA, K. AIHARA, *IEEE Trans.Circuits and Systems-I* 49(1) (2002), pp.28-40.

- [16] R.A.J. MATTHEWS, *Cryptologia* 13(1) (1989), pp.29-42.
- [17] S. PAPADIMITRIOU, T. BOUNTIS, S. MAVROUDI, A. BEZERIANOS, *Int. J. Bifur. Chaos* 11(12) (2001), pp.3107- 3115.
- [18] Z.-H. GUAN, F. HUANG, W. GUAN, *Phys. Lett. A* 346 (2005), pp.153-157.
- [19] D. XIAO, X. LIAO, K. WONG, *Chaos Solitons Fractals* 23 (2005), pp.1327-1331.
- [20] G.TANG, X.LIAO, Y.CHEN, *Chaos Solitons Fractals* 23 (2005), pp.413-419.
- [21] F.HUANG, Z.-H GUAN, *Chaos Solitons Fractals* 23 (2005), pp.851-855.
- [22] SSEH. ELNASHAIE, ME. ABASHA *Chaos Solitons Fractals* 5 (1995), pp.797-831.
- [23] L. KOCAREV, *IEEE Circ Syst* 1 (2001), pp.6-21.
- [24] VI. PONOMARENKO, MD. PROKHOROV. *Phys Rev E* 66 (2002), pp.026215-21.
- [25] M.A. JAFARIZADEH, S. BEHNIA, S. KHORRAM, H. NAGSHARA, *J, Stat. Phys.* 104(516) (2001), pp.1013-1028.
- [26] M.A. JAFARIZADEH, S. BEHNIA, *J. Nonlinear Math.Phys.* 9(1), (2002), pp.1-16.
- [27] K.-W. WONG, *Phys. Lett. A* 298(4) (2002), pp.238-242.
- [28] K.-W. WONG, S.-W. HO, C.-K. YUNG, *Phys. Lett. A* 310 (2003), pp.67-73.
- [29] T. XIANG, X. LIAO, G. TANG, Y. CHEN, K.-W. WONG *Phys. Lett. A* 349 (2006), pp.109-115.
- [30] G. CHEN, Y. MAO, C.K. CHUI. *Chaos Solitons Fractals* 21 (2004), pp.749-761.